1st Year Report - Searching for UHE Neutrinos Using ANITA

Matthew Mottram
University College London

Abstract

This report summarises the work I have carried out so far for the ANITA project. I have investigated possible hardware trigger alterations, which would be made before launching ANITA for its second full flight in the Austral Summer of 2008-09. I have also performed checks to ensure that the prioritizer software used during the flight works as intended. In addition I have familiarised myself with the ANITA I data, producing a series of power spectra that neatly summarise the majority of observed events.

June 3, 2008

1 Introduction

The detection of ultra-high energy (UHE) cosmic rays (energies of 10^{17}eV upwards) has been of interest to particle and astrophysicists for a number of years. These particles, with energies many orders of magnitude in excess of those attainable by terrestrial particle accelerators, are products of some of the most exotic processes in the Universe. The detection of sufficient cosmic rays at such high energies would enable physicists to test and develop fundamental particle physics theories at energies unaccessable via any other means. Valuable information regarding both the production mechanisms of these particles, the physical processes occurring within the sources would also be obtained. Unfortunately, a combination of effects severely hampers physicists' ability to observe UHE cosmic rays.

The cosmic ray flux drops rapidly with energy (figure 2[1]), so that at 10^{19}eV there will be approximately 1 particle per km^2 per year. It is predicted that this already low flux is decreased further due to interactions that are only possible at such high energies. Protons (which make up the vast majority of the cosmic ray flux) and atomic nuclei at > 30EeV are able to interact with the cosmic microwave background (CMB) via equations 1 and 2 to produce pions. This process was first theorized by Greisen (1966) and Zatsepin & Kuzmin (1966) and as such is known as the GZK effect. The reactions lead to a path length limit for UHE cosmic rays, resulting in a $\sim$50Mpc horizon for protons (much lower for heavier nuclei) beyond which cosmic rays will not be observed. There are currently a number of experiments observing cosmic rays at energies up to and beyond the GZK cutoff, a number of which display evidence of the predicted lowering in flux due to the GZK effect. The measured cosmic ray spectrum from the HiRes experiment is displayed in figure 2, the dip in flux at energies above 10^{19}eV is noticable, although results from other experiments, such as AGASA, do not observe this feature.

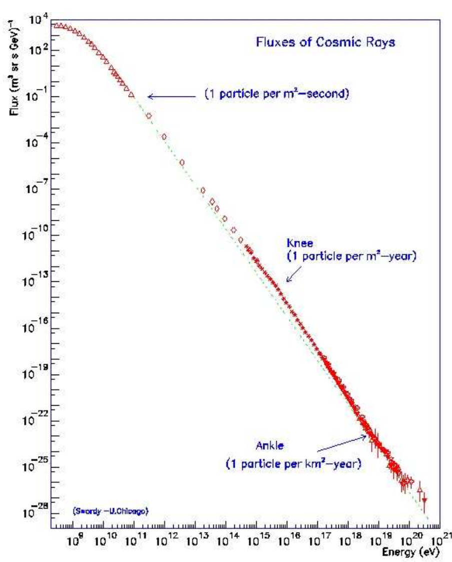

Figure 1: Cosmic ray flux.

[1]http://astroparticle.uchicago.edu/sciam1.jpg

$$\gamma + p \rightarrow \Delta^+ \rightarrow \pi^0 + p \tag{1}$$

$$\gamma + p \rightarrow \Delta^+ \rightarrow \pi^+ + n \tag{2}$$

In a similar fashion to cosmic rays, UHE γ rays begin to be attenuated at high energies, when pair production via interaction with the cosmic infra-red background (CIB) becomes possible. Again, this creates a detection horizon that is seriously detrimental to the usefulness of the γ ray in solving astrophysical issues at the UHE level.

Therefore, at UHE energies, physicists require an alternative observable to the two most commonly used astrophysical messengers. The hope is that this third high energy particle would provide a missing link that would tell us about the composition of the UHE cosmic ray flux, which in turn would allow advances in descriptions of production mechanisms and test our understanding of particle physics at these energy levels.

A solution to the observation problem lies with neutrinos. Neutrinos carry no electric charge, have negligible mass and interact only via the weak nuclear force with a very small interaction cross section. Because of this they will travel almost uninterrupted and will always point back to their source (unlike cosmic rays which may be deflected by, e.g., electric fields). So neutrinos from, for example, AGN could provide uncontaminated information on production rates and energy spectra of the source.

An additional and much more detectable source of UHE neutrinos would be those created by the decay of GZK pions from equations 1 & 2. A flux of these GZK neutrinos is inevitable due to the unstable nature of the pion whose decay will lead to lepton production. Detection of the neutrinos would not only further confirm the GZK process, but also allow us , at the very least, to place limits on the flux for GZK cosmic rays. This would provide us with an idea on the cosmic ray content (e.g. the amount of iron nuclei) at high energies.

Unfortunately, the fact that neutrinos are such good astrophysical messengers also makes them incredibly hard to detect on Earth. Add into this the fact that their flux is

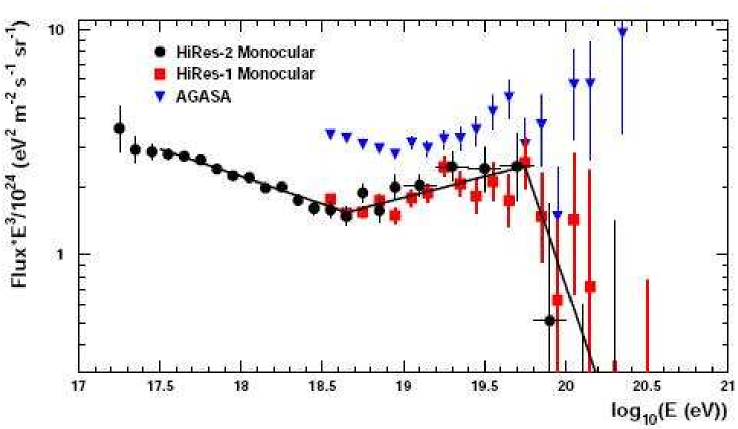

Figure 2: UHE cosmic ray spectrum as observed by HiRes and AGASA (HiRes Collaboration 2007).

already low, as dictated by the cosmic ray flux, and it is found that an incredibly vast amount of detector material is required if we are to observe UHE neutrinos.

At present there are a number of neutrino detectors operating in the TeV energy range. These experiments use large detector volumes (km^3 of ice or water) to search for Cherenkov light created by secondary particles created when the neutrinos interract. However, current optical Cherenkov neutrino detectors, such as IceCube in Antarctica, are unable to observe the volume required to put a sensible limit on the UHE neutrino flux. Also, as optical light has a relatively short attenuation length in ice, to scale some detector such as IceCube up to the size where it may be able to look for UHE neutrinos is totally unfeasible.

2 Askaryan Effect

A method by which particle showers could be observed in a dielectric medium such as ice was suggested by Askaryan (1962). The process, known as the Askaryan effect, produces observable Cherenkov radiation at radio frequencies.

If, for example, a 10^{18}eV neutrino interacts in ice, the resultant particle shower will contain on the order of 10^7 electrons and positrons at the shower maximum, with a bunch size a few cm wide and ∼1cm thick. The shower will develop over a region of a few metres from the initial interaction vertex and, because of e^+ annihilation with non-shower e^-, as well as further e^- being added to the shower via the Compton effect (equations 3 & 4), will have a negative charge imbalance of ∼20%. Cherenkov emission from this shower will therefore be coherent at wavelengths larger than the transverse size of the shower (> few cm).

$$e^+ + \text{rest}\, e^- \rightarrow \gamma + \gamma \tag{3}$$

$$\gamma + \text{rest}\, e^- \rightarrow \gamma + \text{shower}\, e^- \tag{4}$$

The total Cherenkov radiation energy emitted by one particle over a path length L is defined by equation 5. Here, c is light speed, h is Planck's constant, α is the fine structure constant ($\sim 1/137$), n is the dielectric constant for the interaction medium, β is the charged particle's velocity/c and ν_{min} to ν_{max} is the frequency range over with the power is emitted.

$$\omega = \left(\frac{\pi h \alpha}{c}\right) L \left(1 - \frac{1}{n^2\beta^2}\right)\left(\nu_{max}^2 - \nu_{min}^2\right) \tag{5}$$

For N excess charged particles in a shower the total power in this frequency range scales with N^2 (equation 6). This means that a particle shower with $>10^6$ excess electrons (typical for a 0.1EeV neutrino interaction) will produce $>10^{12}$ times more power in radio frequencies than a single charge. The result will be a detectable signal, created over a relatively broadband range of radio frequencies (figure 3).

$$\Omega = N^2\omega^2 \tag{6}$$

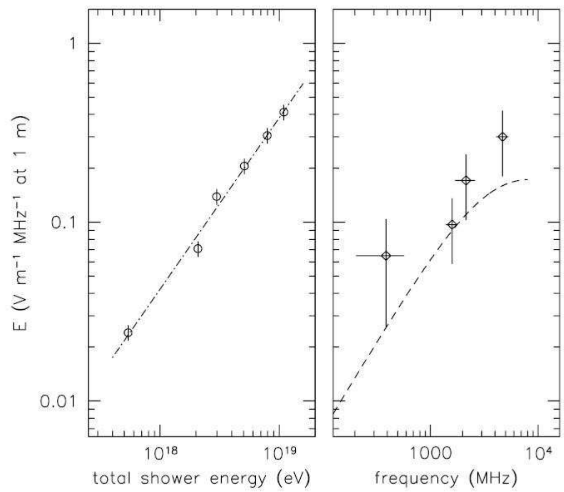

Figure 3: Plots of measured (*data points*) and predicted (*dashed curves*) electric field strength at 2.1GHz (*left*) and spectral dependence of electric field strength (*right*) for Askaryan pulses in silica sand (Saltzberg et al. 2001).

Although theorized in 1962, the Askaryan effect has only recently been confirmed experimentally. The first detection of an Askaryan pulse was made by Saltzberg et al. (2001), using silica sand as the dielectric medium. The process has been further confirmed in ice (Gorham et al. 2007) which, existing in such large quantities at both poles of the Earth, and having large attenuation lengths of radio frequencies, could provide the ideal interaction medium for observations of UHE neutrinos.

3 The ANITA Instrument

Although the Askaryan effect is seen as a possible solution to many of the problems in UHE particle and astrophysics, the issue of requiring large volumes of interaction material remains. The attenuation length of radio frequencies in ice is on the order of kilometres, but scaling up the idea of current ground based optical detectors to produce a ground based radio detector will still require enormous investment.

ANITA was proposed as pathfinding experiment with the intention of investigating the feasibility of further radio Cherenkov detectors, whilst having a primary goal of becoming the first experiment to detect UHE neutrinos. In the event that none of these particles are observed, ANITA will still be able to set the most sensitive limit yet on the UHE neutrino flux (figure 4). Designed as a balloon borne experiment, ANITA is able to observe a vast volume of Antarctic ice without being prohibitively expensive. To date ANITA has completed two flights, one as ANITA-lite, a scaled down two antenna version of the full model which completed an 18 day flight in 2003-04, and a full 35 day flight in 2006-07.

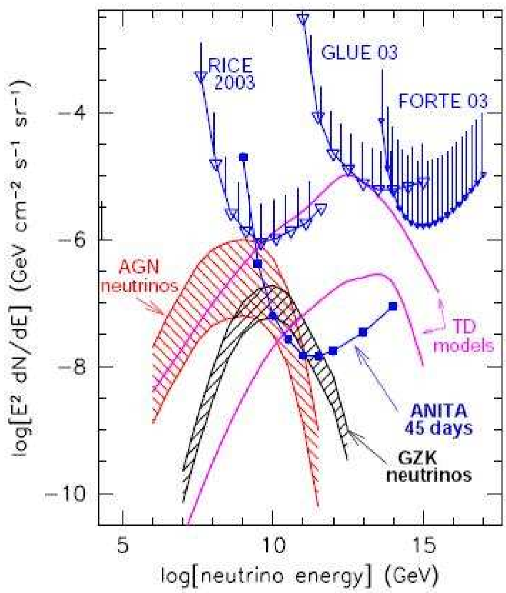

Figure 4: Published sensitivities from radio UHE neutrino detectors RICE and GLUE along with a projected sensitivity for 45 days of ANITA data (Miocinovic et al. 2005).

3.1 Basic Design

The instrument itself comprises of a 360° array of quad-ridge radio horn antennas, with 32 antennas total in the 2006-07 flight and a further 8 planned for the 2008-09 flight (figure 5[2]). Each antenna has a slight downward cant of 10° which, when flying at an altitude of 36km, allows signals out to the horizon of 700km to be observed. It is possible for ANITA to observe a maximum total area of $>1.5\times10^6$km^2 and volume of $>1.5\times10^6$km^3 of Antarctic Ice.

The slight downward pointing of the antennas allows for them to view to within 40° of the nadir. This is sufficient as, at the energies being investigated, neutrinos have a a large enough cross section for any upgoing flux to be totally absorbed. As downgoing neutrinos are also not observed by ANITA the ones the experiment hopes to see are 'skimmers' - within ±15° of 0° declination (figure 6).

In order for ANITA to be able to fully utilise the vast observable interaction volume, its design has ensured that there are no blind spots in the full 360° coverage. The radio antennas have a beamwidth of 60° - 70° over all operating frequencies, allowing for overlap with their neighbours.

The frequency range ANITA operates in, 200MHz - 1200MHZ, reflects the broadband nature of Askaryan signal and is a key to removal of noise. The upper observation frequency limit of ∼1200MHz is chose due to radio Cerenkov radiation no longer being coherent at frequencies much higher than the GHz level (figure 3). The lower frequency limit of ∼200MHz, meanwhile, is imposed by the requirement of overlapping antenna beams and the maximum possible gondola size. The design of ANITA's antennas means that

[2]http://www.hep.ucl.ac.uk/∼rjn

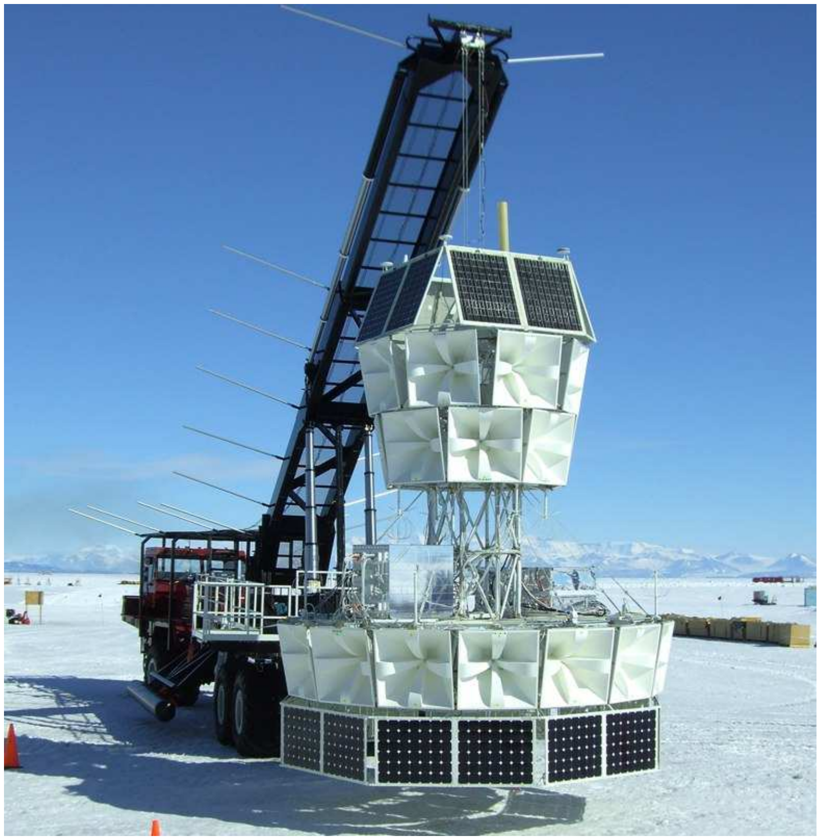

Figure 5: The ANITA I instrument.

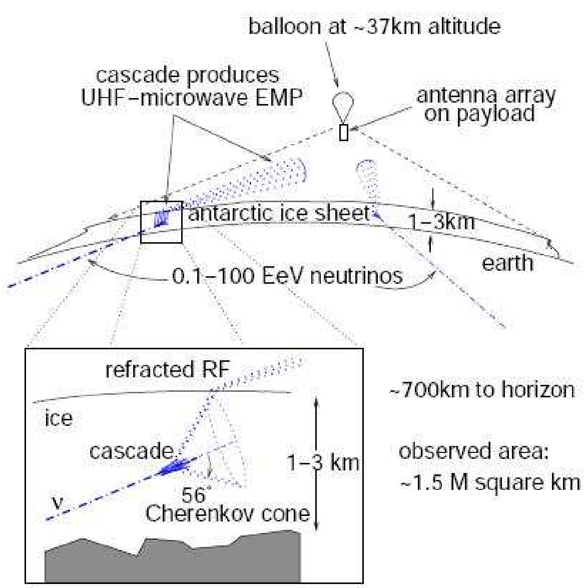

Figure 6: A schematic of ANITA detecting a neutrino event (Gorham et al. 2003).

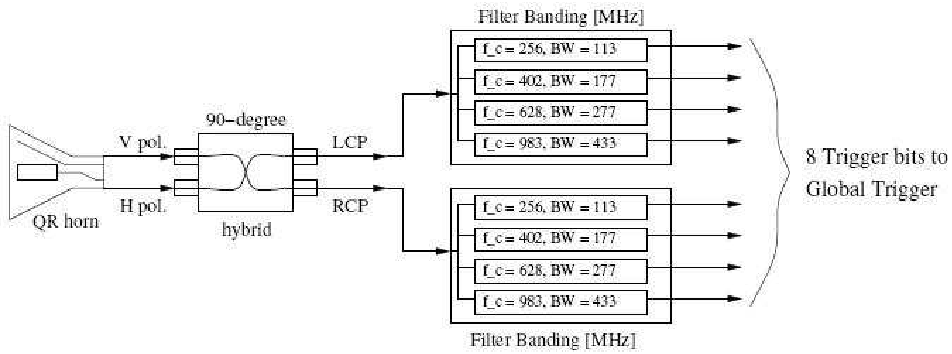

Figure 7: The ANITA I frequency banding and level 1 trigger (Varner et al. 2004). 3 of 8 channels triggering passed level 1.

these radio frequencies are received in both horizontal and vertical polarizations (H-POl and V-POL).

The 2 level split in antenna distribution allows for the calculation of a signal's elevation angle, achieved by pulse timing with a 0.2° resolution at the horizon. The azimuthal angle, meanwhile, is calculated via the ratio of signal pulse amplitudes in neighbouring antennas, with a 0.8° resolution.

To locate signal sources differential GPS is used measure the pitch, roll and heading of the payload, with backup provided by Sun sensors, magnetometers and accelerometers. Power is drawn from photovoltaic cells and event data is stored on board the instrument, with a small fraction of events also transmitted via satellite link to ground.

3.2 Triggering

Radio signals that are recieved by the antennas are amplified and sent through bandpass filters producing the 200-1200MHz frequency range. This range is then filtered into a number of sub-band ranges (with the option of retaining a full band as well) upon which a hardware trigger operates using tunnel diodes.

1 - Single antenna (Level 1): Analogue information from each antenna is provided in two polarizations (vertical and horizontal which can be combined to give left and right circular) as well as the banded frequency channels. For ANITA I, 4 frequency sub-bands were used with circular polarizations, giving 8 channels per antenna in total (figure 7). Any signal triggering on 3 of these 8 channels (within a time coincidence window) or more was passed onto the next trigger level.

2 - Antenna cluster (L2): 2 of 3 adjacent antennas must be pass level 1 for level 2 triggering to be satisfied.

3 - Phi sectors (L3): The upper and lower levels of antennas can be divided into 16 phi sectors with one antenna from each of the top and bottom antenna rings comprising a phi sector (figure 5). To pass this final trigger stage there must be L2 triggers in the same phi sector for both upper and lower levels of antennas.

To maintain a constant global trigger rate, the trigger thresholds for each polarisation and antenna are variable. So, if the trigger rate in a certain channel is high relative to the desired rate, then the corresponding threshold can be increased.

Events passing the hardware trigger are digitised and stored on board ANITA. As well as basic waveform and timing data, GPS data is recorded and stored, along with further information on the global and local event rates, trigger thresholds etc.

4 Physics Contribution

4.1 Hardware Trigger Analysis

As mentioned in the previous section, ANITA has three levels of hardware triggering. During ANITA I signals received in V-POL and H-POL were first converted to information in circular polarizations. The level 1 trigger was passed if 3 of 8 channels had been triggered. This system was used due to the broadband nature of Askaryan pulses (as a minimum of 2 frequency bands must trigger).

Cherenkov radiation, and so Askaryan radiation also, is totally linearly polarized, with the polarization always perpendicular to the tangent of the Cherenkov cone. Because of this, equal components of radiation will be observed in both left and right circular polarizations. A circularly polarized trigger, therefore, seemed the most sensible for ANITA I. However, the amplitude of any signal will be reduced by a factor of $\sqrt{2}$ when converting to this circular polarization. With a linear polarization, depending on the angle between signal and detector polarization, the signal amplitude may be reduced by a much smaller factor.

For a radio signal to exit ice the signal must have some upgoing component, otherwise total internal reflection would take place. Due to the nature of an Askaryan pulse's polarization, this means any Askaryan pulse detectable by ANITA must have at least some vertically polarized component. Because of this it was deemed necessary to investigate whether a vertical/horizontal polarization trigger combination would be more effective than a circularly polarized one.

Using Amy Connolly's ANITA Monte Carlo (MC), the effective sensitivity of ANITA was calculated for different L1 trigger configurations. As well as looking at the polarization of the triggering, the effect of changing the total number of frequency sub-bands, as well as the number of sub-bands required for a trigger, was looked at. A final option that was tested involved adding an additional trigger on the full-band frequency range. Passing the L1 trigger when only 1 sub-band triggered was not considered. Results using this option with the MC may have displayed good sensitivity to neutrinos, but it is not a viable trigger setup as ANITA would be swamped with narrowband noise triggers that could be both thermally and RF broadcast induced.

The overall trigger rate for ANITA is determined by the maximum speed which digitizing data and writing events to disk is possible. For both ANITA I and ANITA II this maximum global hardware trigger rate limit is 5Hz. Using this final rate, it is possible to calculate the maximum single channel (pre L1) trigger rates using equation 7. Figure 8 then allows for a threshold to be chosen each sub-band trigger based on the rate of thermally induced triggers (the most common triggers ANITA will encounter).

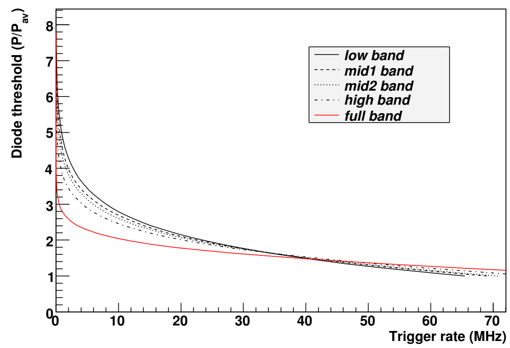

Figure 8: Conversion plot from sub-band trigger rates to diode thresholds. For 3 sub-bands only one of the mid range response curves was used.

$$R_{N,M,\Delta t,r} = \sum_{i=N}^{M} \left[\sum_{j=0}^{i-N} (-1)^j \, C_i^j \right] iC_M^i r^i \Delta t^{i-1} \tag{7}$$

Here R is the upper level trigger rate being calculated and r the lower (e.g. R = L3 rate, r = L2 rate), for a coincidence of N of M channels. Δt is the time coincidence window (11, 5 and 12.5ns for L1, L2 and L3 respectively) and C_i^j is defined by equation 8 (again for coincidences in N of M channels).

$$C = \frac{M!}{N!\,(M-N)!} \tag{8}$$

For rate calculations when an additional full band trigger was required in addition to the N of M sub-band triggers, further stages must be included in the calculation. As the full band is *required*, rather than involved in the N of M, it is essentially included at the L2 trigger stage. Because of this, the single channel rate in the full band will not be the same as the single channel rate in the sub-bands. By finding the L2 rate required for a global trigger rate of 5Hz, and selecting various full band rates, the corresponding sub-band trigger rates can be calculated. This again provides us with trigger thresholds for the sub-bands as well the full band using figure 8.

To obtain sensitivities the ANITA MC was run using 10,000,000 events for each trigger and diode threshold configuration. The neutrinos were produced using a GZK neutrino spectrum and the overall sensitivity of ANITA was then calculated for the chosen setup.

It was found that the majority of linearly polarized setups had a better sensitivity that the ANITA I 3 of 8 configuration. Those with a seqerate full band trigger performed particularly well (figure 9). Increasing the full band trigger threshold, and in turn lowering the sub-band thresholds, seems to further increase the sensitivity to neutrino events. However, these sub-band thresholds cannot be decreased beyond the values shown in figure 9 as the trigger would be constantly activated (equation 7 relies on $r\Delta t$<1).

These results, along with others from investigations carried out by other members of the ANITA collaberation, have demonstrated that the hardware trigger can definitely be

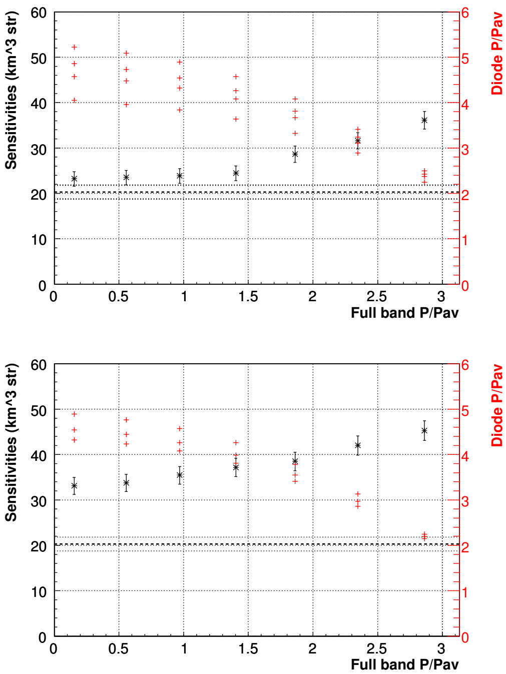

Figure 9: Sensitivity plots for L1 trigger configurations of 2 of 4 (*top left*), 3 of 4 (*top right*) and 2 of 3 (*bottom left*) all using only V-POL triggering. Each configuration had a required full band trigger. Diode thresholds for the sub-bands are displayed for each full band diode thresholds, with the highest thresholds always being that of the high frequency band and the lowest that of the low frequency band. For each configuration the lower the sub-band thresholds, the better the sensitivity, with the 2 of 3 configuration performing the best. The 3 of 8 sensitivity and its errors are displayed by the dashed black lines on each plot.

optimised from the one used in ANITA I. When ANITA II begins taking data it will use a purely linearly polarized trigger. While horizontally polarized data will still be recorded, only vertically polarized signals will be triggered on, a decision that is supported by the results in figure 9. The chosen setup will include modified frequency banding, with only 3 frequency sub-bands and a L1 hardware trigger that is activated when 2 of these bands are triggered.

4.2 Prioritizer

A risk to ANITA that must be taken into account, however unlikely, is that an event may cause the loss of all stored data onboard the gondola. This could occur, for example, in the case that the balloon lands offshore. Because of this and the need to observe ANITA events during flight to ensure data is being taken as intended, ANITA maintains a satellite link during flight over which data is transmitted for storage. While the global hardware trigger passes events of ∼15kByte at a constantly maintained 5Hz, the satellite link can only transfer data at a maximum of 6kbit/s. Therefore it is only possible for about 1 in 150 of the triggered events to be transmitted.

Lowering the trigger rate by either toughening the cuts on trigger coincidences or raising trigger thresholds is not an option. Loss of background would be detrimental to analysis and, far more importantly, the sensitivity to neutrinos would be dramatically reduced. Instead, once the basic binary event files have been created they are passed though a prioritizer stage. By choosing only the most interesting events to transmit it is possible to ensure that any neutrino candidate will be retained in the event of onboard loss of data.

The prioritizer inspects and assigns a priority value of 1 (high) to 9 (low) to each event. This priority is based primarily on how many antennas that are either adjacent in the same ring, or are in different antennas rings but corresponding phi sectors, triggered on the event simultaneously. ‘Bad’ events, such as cases where too many antennas (i.e. many antennas, including some that could not possibly ‘see’ the same event) triggering simultaneously are flagged with specificly valued low priorities.

Using an ANITA event generator created by Stephen Hoover it is possible to produce simulated volt-time waveforms from neutrino events for each ANITA antenna and polarization. Noise is included as standard in the event generator, with a reasonable default of 180K (galactic noise & ice temperature). These waveforms can then be fed through the prioritizer (after conversion to a format produced by the digitizer onboard ANITA). A useful addition to the event generator is an option to check if neutrino events manage to pass the hardware trigger.

Figure 10 shows the distribution of priorities for various signal to noise ratios (SNRs) for all and triggered only simulated events. It can be seen that the majority of the 10^{21}eV neutrinos, as well as a small proportion of the 10^{20}ev events, are assigned a priority of 8. It would be expected, as these are neutrino induced signals, that these events are assigned a high priority (low numerically), but this is not always the case for events with an SNR of >6 and almost never the case for events with an SNR of > 10 (figure 11).

A priority of 8 is assigned as a ‘bad’ event flag where pulse peaks are seen by too many different antennas at one time. The intention of this is that events caused by some

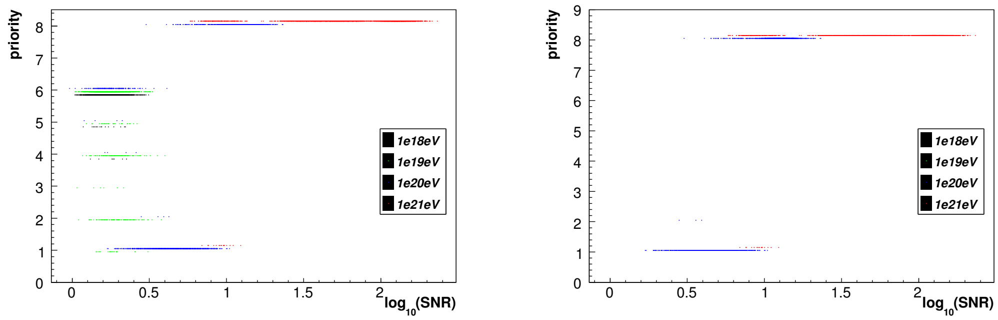

Figure 10: The assigned priority of simulated events (and 180K thermal noise) with varying SNR values is shown for 10^{18}, 10^{19}, 10^{20}, 10^{21}eV events (2000 of each) with all events plotted on the *left* and only triggered events on the *right*. Each pulse was created at a depth of 200m. The varying SNR value was created by applying a random factor between 10^{-6} and 10^{-5} to the signal amplitude at 1m (in place of stating the actual distance between payload and signal).

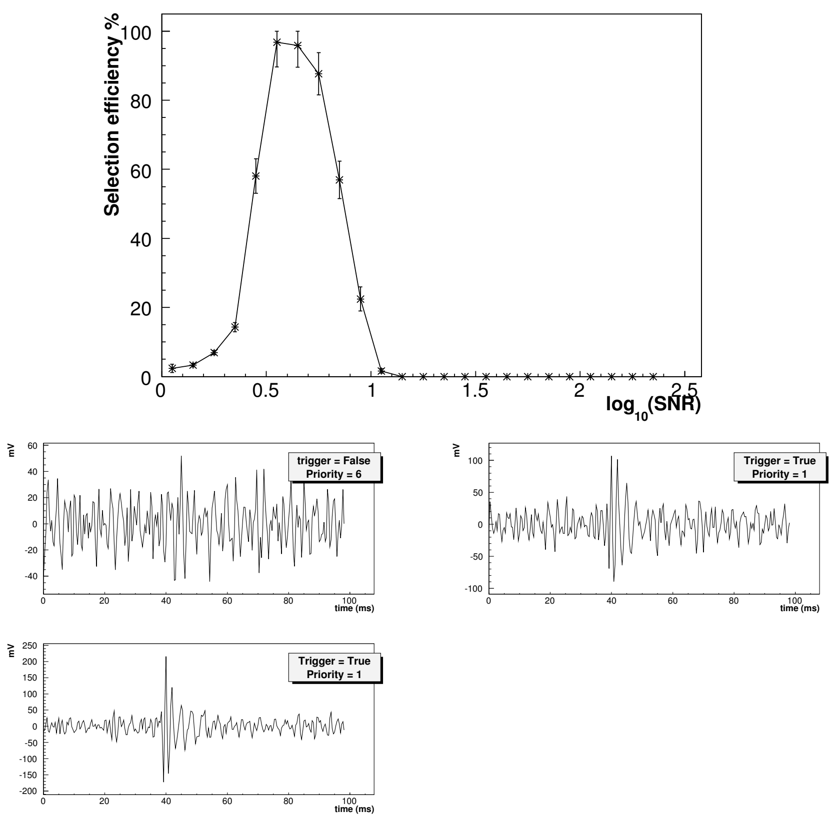

Figure 11: The percentage of simulated events (both those that passed and failed the hardware trigger) that are assigned a priority of 4 or less. Example simulated events with SNR values of 1.25, 3.15 and 7.95 are also shown.

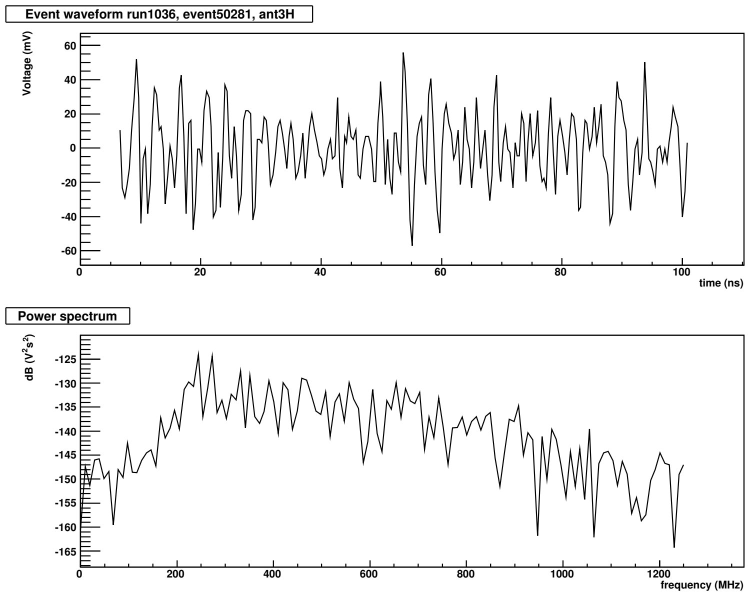

Figure 12: A randomly selected waveform from a random antenna is shown for an ANITA event (*top*). In order to create the power spectrum for the event, any bad time bins (i.e. time values that do not increase consecutively in value) are removed, and the event is interpolated. A fast Fourier transform is then implemented to create a V^2s^2 power spectrum.

electronics glitch, or a very strong (non-neutrino) source, will be assigned a low priority. Simulated waveforms from neutrinos of 10^{20} and 10^{21}eV at reasonable distances from the payload regularly provide an SNR greater than 2 in more than 8 channels. These events are almost always assigned a priority of 8.

It is clear that this 'max number of horns' flag in the prioritizer will have to be altered for ANITA II. The number could simply be increased, or a method could be used that assigns the event a bad priority flag only if antennas on opposite sides of the payload receive a pulse simultaneously.

Further checks on the prioritizer have been carried out. The priority value's dependence on signal direction has been looked at, with no effect having been observed. Thermal noise with no signal has also been used in the range 150-250K, no effect on the priority was seen and no events passed the hardware trigger. Additional prioritizer studies are ongoing, with thermal noise & neutrino signal events being used as well as plans to use outputs of the ANITA MC with the signal generator and prioritizer.

4.3 Power Spectra

Aside from analysis to improve aspects of ANITA II relative to ANITA I, I have also familiarised myself with the format of data from the first ANITA flight. The product of this work is a series of power spectra graphs and histograms documenting the nature of typical events (including, for example, triggered thermal noise) seen by ANITA throughout its first flight.

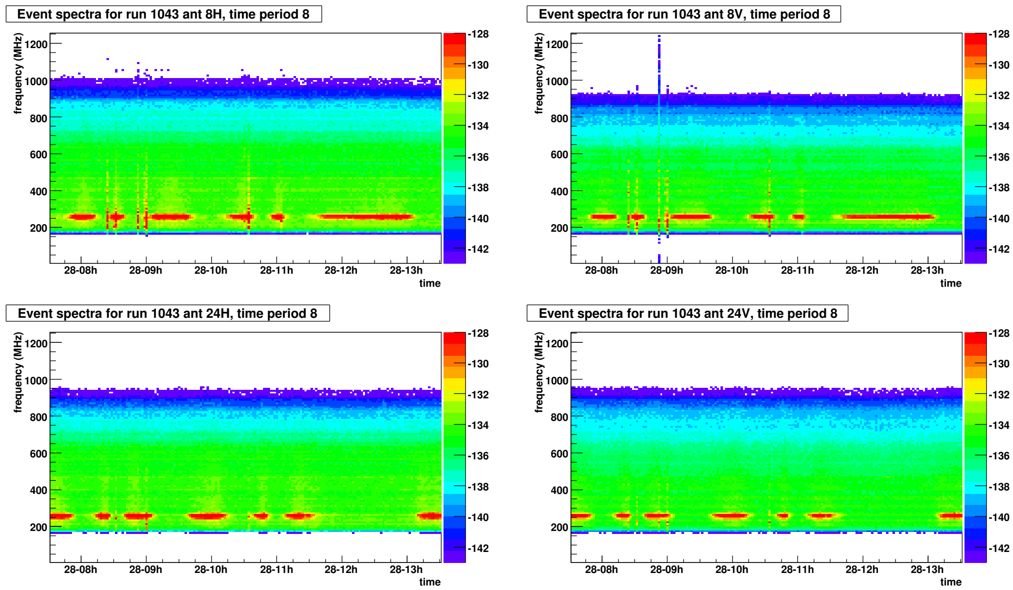

Figure 13: Power spectra histograms are shown for run 1043, timeperiod 8, with antenna 8 H-POL (*top left*) and V-POL (*top right*) and antenna 24 H-POL (*bottom left*) and V-POL (*bottom right*). The colour axis displays the power in dB(V^2s^2). Power spectra are created for each event, as in figure 12. The constant noise at ~260MHz is seen as an isolated source - as antenna 8 and 24 are on opposite sides of the payload, and the noise is never seen by both antennas simultaneously. The plots also demonstrate the increased power received through H-POL relative to V-POL.

Figure 12 shows a typical waveform as recorded by ANITA and its corresponding power spectrum. A power spectrum like this was created for every for each antenna and polarization for every ANITA event. Average power spectra were then created for each run of data, again for every antenna and polarization, as well as an average over all antennas & polarizations. The power spectra histograms, meanwhile, were created by averaging event power spectra over 2 minute periods, then plotting these over 6 hour periods. It should be noted that while only a fraction of the antennas will have been triggered for any one event, data on the signal received through every antenna and polarization was recorded and included in the power spectra plots.

Examples of the histograms are displayed in figures 13 and 14. All of the plots show that the strongest source types seen during the flight are isolated radio emitters, with both ground based and satellite sources observed.

One of these sources appears constantly throughout the ANITA I flight (though it is not always the strongest isolated noise source). Because of its constant appearance throughout the flight, and the fact the the power received does not alter with time, the source of the noise must be satellite based. Similar noise was observed with ANITA-lite and it has been suggested that a notch filter be implemented to cut out this noise during the ANITA II flight. However, the ill effect this would have on ANITA's neutrino sensitivy is too large for any such filter to be included onboard ANITA. The fact that this 260Mhz noise appears to be stronger in H-POL compared to V-POL may be a small encouragement for ANITA II because of the use of V-POL only triggering.

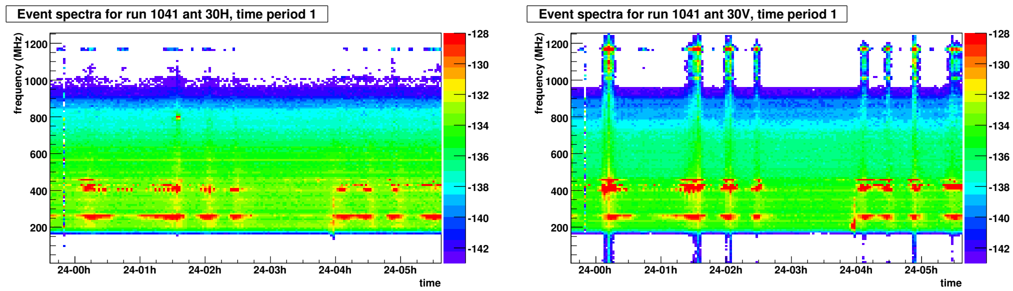

Figure 14: It is also possible to see when ANITA may have been over a ground based radio transmitter using the power spectra. The two plots show an increase in received power, that again appears to be from an isolated source, at ∼450MHz and also (V-POL only) ∼1200MHz. The ground based nature is suggested by the 1200MHz source appearing in ANITA data in run 1039 and remaining in view only for 30 hours. Also, while the timing of the signal appears to be in phase with the 260MHz noise, this is not the case for the entire 30 hour period.

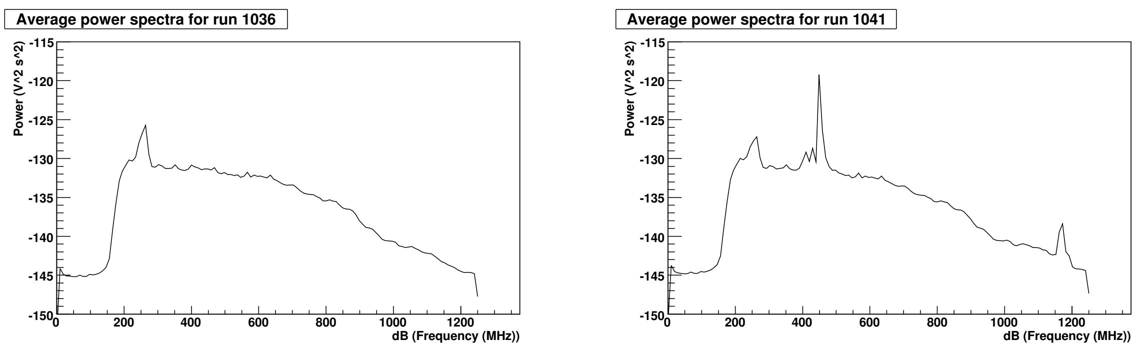

Figure 15: Event, antenna and polarization averaged power spectra are shown for two ANITA data runs, both containing over 500,000 events.

Figure 15 shows two examples of the event averaged power spectra for two data runs (1036 and 1041). These examples are also averaged over all of the antennas and polarizations, so give a very general view of the nature of events being observed. The noise at 260MHz is noticable in both plots, with the 1041 power spectrum also displaying noise (probably ground based) at 450MHz.

The response of the antennas over the operating frequency range can be observed in these graphs and the event histograms. At frequencies below 200MHz there is no response, which is expected as a bandpass filter has been used. The response of ANITA at high frequencies also appears to drop off gradually.

4.4 Additional work

Further to the work outlined above, in March-April of this year I visited the University of Hawaii at Manoa. It is there that most of the work on the gondola, as well as a large amount on the electronics and software development, is being carried out. During the visit I worked on various aspects of the ANITA construction and testing. These tasks mainly included electronics work, for example helping to construct the first stage filtering and amplifying modules, as well as designing small sections of the ANITA electronics box.

5 Future Plans

5.1 Short Term

In terms of short term objectives, the most important part of my work is to assist in preparations for the ANITA II flight. This includes completing the prioritizer studies and any further software checks and analysis.

This June ANITA will be transported in sections from the various collaborating institutions to Palestine, Texas, so that pre-flight tests and instrument integration can be carried out. Work here will last for approximately 6 weeks and I will be present for majority of this time.

5.2 Long Term

The long term the aim of my PhD is to carry out analysis on the ANITA II data, which is to be collected in the Winter of 2008-09. This will involve developing my own analysis code, the result of which will allow me to assist with the ANITA collaberation's aim of detecting the first neutrino in the 0.1-100EeV range. If, after two ANITA flights, no neutrinos are detected then we will still be able to place a limit on the GZK neutrino flux with a sensitivity that will be an improvement of two orders of magnitude over all previous experiments.

References

Askaryan, G. A. 1962, JETP, 14, 441
Gorham, P. W. et al. 2003, ANITA proposal
—. 2007, Phys. Rev. Lett., 99, 171101
Greisen, K. 1966, Phys. Rev. Lett., 16, 748
HiRes Collaboration. 2007, ArXiv Astrophysics e-prints
Miocinovic, P. et al. 2005, ArXiv HEP e-prints
Saltzberg, D. et al. 2001, Phys. Rev. Lett., 86, 2802
Varner, G. S. et al. 2004, note 04-002 ANITA E-LOG
Zatsepin, G. T. & Kuzmin, V. A. 1966, JETP Lett., 4, 78